

Diagnostic capacity of the keratoconus match index and keratoconus match probability in subclinical keratoconus

Georgios Labiris, MD, PhD, Athanassios Giarmoukakis, MD, Zisis Gatzoufas, MD, PhD, Haris Sideroudi, PhD, Vassilios Kozobolis, MD, PhD, Berthold Seitz, MD, PhD

PURPOSE: To evaluate the diagnostic capacity of the Ocular Response Analyzer's keratoconus match index (KMI) and keratoconus match probability (KMP) classification in keratoconus-suspect eyes.

SETTING: Department of Ophthalmology, University Clinics Saarland, Homburg, Germany.

DESIGN: Comparative case series.

METHODS: The KMI and KMP parameters in keratoconus-suspect eyes and normal eyes (control group) were compared. The quantitative keratoconus percentage index was calculated for all suspect eyes. According to the thinnest corneal thickness (TCT), keratoconus-suspect eyes were divided into 2 subgroups: subgroup 1 (TCT <520 μm) and subgroup 2 (TCT >520 μm). The KMI's overall predictive accuracy was assessed using receiver operating characteristic (ROC) curves. The relationship between KMI and a series of Scheimpflug-derived keratoconus-related indices was evaluated using Spearman analysis.

RESULTS: The mean KMI was 0.41 ± 0.29 (SD) in the keratoconus-suspect group (50 eyes) and 0.94 ± 0.29 in the control group (50 eyes) ($P < .001$). Nonsignificant KMI differences were detected between the keratoconus-suspect subgroups (subgroup 1, 27 eyes; subgroup 2, 23 eyes) ($P = .059$). Nonsignificant correlations were found between Scheimpflug indices and the KMI. The KMP identified 27.65% of control eyes as keratoconus suspect and 10.71%, 28.57%, and 3.57% of keratoconus-suspect eyes as being normal, having mild keratoconus, or having moderate keratoconus, respectively. The ROC analysis for the KMI indicated a predictive accuracy of 94% (cutoff point 0.72).

CONCLUSIONS: The KMI seems to be a valuable index in the early diagnosis of keratoconus-suspect eyes. The KMP identified a significant percentage of topographically defined keratoconus-suspect eyes as normal or keratoconic.

Financial Disclosure: No author has a financial or proprietary interest in any material or method mentioned.

J Cataract Refract Surg 2014; 40:999–1005 © 2014 ASCRS and ESCRS

Keratoconus is a progressive noninflammatory bilateral ectatic corneal disorder. Its incidence is estimated as approximately 1 per 2000 in the general population,^{1,2} with higher incidences reported in refractive surgery candidates.^{3,4} In most cases, keratoconus starts during puberty and its rate of progression varies.^{1,5}

Despite keratoconus' well-defined clinical signs, the early forms of the disease present diagnostic challenges. Keratoconus suspects represent subclinical cases of keratoconus with significant importance, especially in

refractive surgery because of its association with ectasia after laser in situ keratomileusis.^{3,6,7} Despite recent scientific efforts to design detection models for keratoconus suspects,^{8–11} specific diagnostic and/or therapeutic guidelines have not been introduced.¹²

Results in former studies^{13–15} indicate the distinct biomechanical properties that keratoconic eyes possess. Keratoconic eyes are known to be more elastic and less rigid and present with less hysteresis than normal eyes.^{13–15}

The Ocular Response Analyzer (Reichert Technologies), a dynamic bidirectional applanation device, is the first commercially available instrument enabling the measurement of the corneal biomechanical parameters of corneal hysteresis (CH) and the corneal resistance factor (CRF) in clinical settings. Numerous studies^{16–20} have attempted to identify the diagnostic potential of CH and the CRF in keratoconus and subclinical keratoconus. The most recent version of the dynamic bidirectional applanation device's software (3.x) enables the measurement of 2 new keratoconus-specific parameters that are based on the distinct waveform characteristics of keratoconic eyes derived by the device. The new parameters are the keratoconus match index (KMI), which is the outcome of a neural network calculation of 7 waveform scores and represents the similarity of the waveform of the examined eye against the same average waveform scores of the keratoconic eyes in the machine's database, and the keratoconus match probability (KMP), which attempts to quantify the probability that a certain eye is normal, suspect, or keratoconic. An extensive literature review found only 1 study of the diagnostic capacity of these contemporary keratoconus-related indices.²¹

Scheimpflug imaging is among the most prevalent modalities for the diagnosis and follow-up of keratoconus eyes and keratoconus-suspect eyes.^{9,11,22,23} It is based on a rotating camera and a monochromatic slit light source that rotate together. In addition to topographic, pachymetric, and elevation maps, the system's software provides a series of keratoconus-related indices that are commonly used in clinical settings.

Within this context, the primary objective of this study was to evaluate the diagnostic capability of KMI and KMP indices in keratoconus-suspect eyes and to explore their association with a series of Scheimpflug camera-derived keratoconus indices and corneal biomechanical parameters.

PATIENTS AND METHODS

This prospective nonintervention study was performed at the Department of Ophthalmology, University Clinics Saarland UKS, Homburg/Saar, Germany, between October 2011 and February 2012. The Institutional Review Board, University of Saarland, approved the protocol, and all participants provided written informed consent.

Participants

Study participants were recruited from the Cornea Outpatient Service on a consecutive (if eligible) basis. Two study groups were formed. The keratoconus-suspect group comprised patients characterized as keratoconus suspects. Inclusion criteria for enrollment in the keratoconus-suspect group were a diagnosis of keratoconus in the fellow eye according to the Amsler-Krumeich criteria, a keratoconus percentage index (KISA%) between 60% and 100% in the keratoconus-suspect eye,²³ and lack of keratoconus-related findings or signs on slitlamp biomicroscopy. The control group comprised refractive surgery candidates. Eligibility for participation in the control group was confirmed by a detailed ophthalmologic examination that included consecutive topographies, slitlamp biomicroscopy, and calculation of the KISA% index.²⁴ The keratoconus-suspect group was further divided into 2 subgroups based on thinnest corneal thickness (TCT) measurements as follows: subgroup 1, which had a TCT less than 520 μm , and subgroup 2, which had a TCT greater than 520 μm .

Exclusion criteria in both groups included previous incisional eye surgery, corneal scars and opacities, history of herpetic keratitis, severe eye dryness, current corneal infection, glaucoma, suspicion of glaucoma, intraocular pressure-lowering treatment, pregnancy or nursing, and underlying autoimmune disease.

Data Collection

For all keratoconus-suspect eyes, the quantitative KISA% index was calculated based on Scheimpflug curvature maps published by Rabinowitz and Rasheed.²⁴ The KISA% index quantifies the minimum topographic criteria for the diagnosis of keratoconus and is derived from the following formula:

$$\text{KISA}\% = K \times (I - S) \times \text{Cyl} \times \text{SRAX} \times 100/300$$

where K is the central keratometry, generated by averaging the dioptric power points on rings 2, 3, and 4 of the topographies; I-S is the inferior-superior dioptric asymmetry value calculated by subtracting the mean value of the superior 5 data points 3.0 mm from the center of the cornea at 30-degree intervals (30, 60, 90, 120, and 150 degrees) from the mean value of the 5 corresponding data points along the inferior cornea (210, 240, 270, 300, and 330 degrees); Cyl is the degree of regular corneal astigmatism (simulated K1-simulated K2); and SRAX is the skewed radial axis value, which is an expression of irregular astigmatism occurring in keratoconus. The SRAX value is calculated by the following formula:

$$\text{SRAX} = 180 \text{ degrees} - \phi$$

where ϕ is the smaller of 2 angles; that is, the angle of the steepest radius above the horizontal meridian and the angle of the steepest radius below the horizontal meridian.

Submitted: November 2, 2012.

Final revision submitted: August 8, 2013.

Accepted: August 9, 2013.

From the Department of Ophthalmology (Labiris, Gatzioufas, Seitz), University Medical Center of Saarland UKS, Homburg/Saar, Germany; the Eye Institute of Thrace (Labiris, Giarmoukakis, Sideroudi, Kozobolis), Alexandroupolis, Greece.

Corresponding author: Georgios Labiris, MD, PhD, Ophthalmology Department, University Hospital of Alexandroupolis, 68100 Dragana, Alexandroupolis, Greece. E-mail: labiris@usa.net, glampiri@med.duth.gr.

Each individual index quantifies a topographic feature of keratoconus; thus, when they are multiplied by one another, an abnormality in 1 amplifies the resultant product. In addition to the above, the following rules were applied:

1. To amplify any abnormality, the value 1 was substituted in the equation when a calculated index had a value of less than 1.
2. Only absolute values were used. For example, if the I-S value was -2.0 diopters (D), it was corrected to 2.0 D; therefore, there were no negative values in the KISA%.
3. The K value that was used was in excess of 47.2 D (ie, $K - 47.2$). For values less than 47.2 D, a value of 1.0 was substituted in the calculation. A KISA% index value greater than 100% was considered early keratoconus; less than 60%, normal; and between 60% and 100%, suspected keratoconus.²⁴

All measurements taken with the dynamic bidirectional applanation device (software version 3.01) were performed by the same experienced operator in a consistent way. Specifically, the patient sat on a chair in front of the device. When the patient's eye successfully fixated on a red blinking target, the operator activated the device. An air puff was released by a noncontact probe, which scanned the central area of the eye and sent a signal to the dynamic bidirectional applanation device. In brief, the air puff caused the cornea to move inward, past applanation, and into slight concavity. After milliseconds, the air pump shut off, the pressure decreased, and the cornea returned to its normal state. The system monitored the entire process and produced a specific waveform. Three consecutive measurements were obtained, and the mean values of all parameters were calculated. When the measurements were of low quality (waveform score $< 8/10$), the procedure was repeated until the acceptable criteria were met. Both keratoconus-specific indices (KMI and KMP) and corneal biomechanical parameters (CH and CRF) were included in the analysis.

Accordingly, the same operator performed all topographies using a Scheimpflug camera (Pentacam HR, Oculus Optikgeräte GmbH). Three consecutive scans were obtained, and the mean values of all parameters were calculated. Acceptable maps had at least 10.0 mm of corneal coverage. Moreover, images with extrapolated data in the central 9.0 mm zone were excluded. For the measurements, patients were asked to blink and then look at the fixation device. When an image was of low quality (lid closure, insufficient fixation or corneal coverage), the procedure was repeated until the acceptable criteria were met. The following keratoconus indices were included in the analysis: keratoconus index; index of vertical asymmetry; index of surface variance; index of height asymmetry; index of height decentration; smallest radius; maximum elevation value in the central 5.0 mm (PEL); corneal volume at 3.0 mm (CV3), at 0.5 mm (CV5), and overall (CV); average pachymetric progression index (PPIavg); Ambrosio relational thickness (ARTavg); central corneal thickness (CCT); TCT; TCT:CCT ratio; and KISA% index.

Statistical Analysis

Normality of the measured data was assessed with Kolmogorov-Smirnov testing, and parametric or nonparametric tests were applied accordingly. Differences between groups were evaluated using the Welch modified Student

2-sample *t* test and Wilcoxon signed-rank test according to the normality of distribution of each parameter.

Receiver operating characteristic (ROC) curves were applied to determine the overall predictive accuracy of the KMI parameter, as described by the area under the curve (AUC). These curves are obtained by plotting sensitivity versus 1-specificity, which is calculated for each value observed. An area of 100% implies that the test perfectly discriminates between groups. This approach was also used to identify the cutoff point for KMI to maximize sensitivity and specificity in discriminating keratoconus-suspect corneas from normal corneas.

The relationship between the Scheimpflug-derived keratoconus-related indices, CH, the CRF, and the KMI was assessed using Spearman analysis. A *P* value less than 0.05 was considered statistically significant. All statistical analyses were performed with Medcalc software (version 9.6.2.0, Medcalc Software bvba).

RESULTS

Table 1 compares the biomechanical and topographic characteristics between groups and subgroups. The CH and CRF parameters were statistically significantly lower in the keratoconus-suspect group than in the control group (both $P < .001$, Mann-Whitney *U* test). The only statistically significant differences in the Scheimpflug camera parameters between the study groups were in the keratoconus index, PEL, CV3, CV5, PPIavg, ARTavg, and TCT/CCT (all $P < .05$, Mann-Whitney *U* test).

There was a statistically significant difference in the KMI parameter between the control group and the keratoconus-suspect group, keratoconus-suspect subgroup 1, and keratoconus-suspect subgroup 2 (all $P < .001$, Mann-Whitney *U* test) (Table 1).

Table 2 shows the KMP distribution in the 2 study groups and 2 subgroups. Thirty-six eyes and 14 eyes in the control group were identified as normal and as suspect, respectively. None was identified as ectatic. Regarding keratoconus-suspect eyes, 7 were identified as normal, 27 as suspect, and 16 as keratoconus.

Table 3 and Figure 1 show the ROC data for corneal parameters by groups and subgroups.

Table 4 shows the correlation analysis in the keratoconus-suspect group. Spearman analysis showed a statistically significant, but moderate correlation between the KMI and the CRF only ($r = 0.41$, $P = .03$). No correlation was found between the KMI and any Scheimpflug index measured in any group.

DISCUSSION

The Ocular Response Analyzer, a dynamic bidirectional applanation device, introduced a simple and reliable way of measuring corneal biomechanical properties in clinical settings. Specifically, the device's software provides 2 parameters that reflect corneal biomechanical characteristics. One is CH, which

Table 1. Biomechanical and topographic characteristics by group and subgroup.

Parameter	Keratoconus-Suspect Group (n = 50)		Control Group (n = 50)		Keratoconus-Suspect Subgroup 1 (n = 23)		Keratoconus-Suspect Subgroup 2 (n = 27)		P Value
	Mean	SD	Mean	SD	Mean	SD	Mean	SD	
KISA% (%)	83.39	18.71	25.32	18.7	68.92	5.46	95.93	16.94	<.01
CH (mm Hg)	8.8	1.37	10.79	1.77	8.28	1.58	9.26	1.01	<.005 ^{*,†,‡}
CRF (mm Hg)	7.66	1.79	10.18	2.07	7.44	1.18	7.87	2.22	<.001 ^{*,†,‡}
K1 anterior (D)	43.2	1.67	43.45	2.13	44.07	1.46	42.56	1.55	.56
K2 anterior (D)	44.01	1.89	44.57	1.87	44.63	1.91	43.56	1.8	.15
Kmean anterior (D)	43.6	1.72	43.99	1.95	44.35	1.63	43.06	1.62	.3
K1 posterior (D)	-6.1	0.33	-6.16	0.41	-6.18	0.29	-6.042	0.37	.4
K2 posterior (D)	-6.4	0.34	-6.54	0.36	-6.41	0.42	-6.39	0.29	.07
Kmean posterior (D)	-6.24	0.32	-6.12	1.72	-6.29	0.36	-6.22	0.31	.71
CCT (μm)	533.24	41.4	550.25	34.78	495.86	19.24	560.79	29.8	<.001 ^{*,†}
TCT (μm)	518.87	70.92	542.55	39.98	469	80.15	555.63	30.71	<.001 ^{*,†}
ISV	21.54	7.59	19.21	8.83	20.79	4.14	22.12	9.45	.22
IVA	0.18	0.06	0.14	0.09	0.19	0.057	0.18	0.076	.06
KI	1.03	0.026	1.02	0.02	1.04	0.024	1.03	0.03	<.05 ^{*,†}
CKI	1.005	0.01	1.002	0.01	1.004	0.01	1.006	0.01	.42
IHA	5.79	5.87	4.45	4.49	7.43	6.2	4.56	5.47	.3
IHD	0.01	0.008	0.01	0.006	0.014	0.063	0.012	0.009	.18
Rmin (mm)	7.49	0.3	7.43	0.32	7.36	0.3	7.59	0.27	.33
PEL (μm)	9.4	3.3	3.9	2.1	11.2	3.6	9.1	3.1	<.001
CV (mm ³)	56.72	3.01	61.72	3.62	55.3	2.9	57.8	3.15	.49
CV5 (mm ³)	10.8	0.66	11.72	0.73	10.1	0.53	11.4	0.72	<.001
CV3 (mm ³)	3.67	0.23	4.01	0.26	2.9	0.18	4	0.29	<.001
PPIavg	1.11	0.22	0.94	0.11	1.01	0.19	1.15	0.3	<.005
ARTavg	466.13	112.62	539.19	75.91	460.12	111.36	472.36	113.1	.001 [*]
TCT:CCT	0.98	0.05	1	0.01	0.97	0.05	0.99	0.05	<.01 ^{*,†,‡}
KMI	0.41	0.29	0.94	0.29	0.36	0.29	0.49	0.244	<.01 ^{*,†,‡}

ARTavg = TCT/PPIavg; CCT = central corneal thickness; CH = corneal hysteresis; CKI = central keratoconus index; CRF = corneal resistance factor; CV = overall corneal volume; CV3 = corneal volume at 3.0 mm; CV5 = corneal volume at 5.0 mm; IHA = index of height asymmetry; IHD = index of height decentration; ISV = index of surface variance; IVA = index of vertical asymmetry; K1 = keratometry in flat meridian; K2 = keratometry in steep meridian; KI = keratoconus index; KISA% = keratoconus percentage index; Kmean = mean keratometry value; KMI = keratoconus match index; PEL = posterior elevation; PPIavg = average pachymetric progression index; Rmin = smallest radius; TCT = thinnest corneal thickness; TCT:CCT = TCT:CCT ratio

*Significant difference between keratoconus-suspect group and control group
[†]Significant difference between keratoconus-suspect subgroup 1 and control group
[‡]Significant difference between keratoconus-suspect subgroup 2 and control group

represents the difference between 2 applanation pressures; that is, the pressure necessary to flatten the cornea as the device's air pressure increases (P1) and the pressure at which the cornea flattens again as the air pressure decreases (P1), deriving from the viscous

damping of the corneal tissue. The second property, the CRF, is considered to be a better indicator of the cornea's overall viscoelastic response to air pressure and is calculated by the following formula: $P1 - K \times P2$, where $K = 0.7$.¹⁵ Former studies have attempted to

Table 2. Distribution of KMP by group and subgroup.

Parameter	KMP Distribution (%)			
	Keratoconus-Suspect Group	Control Group	Keratoconus-Suspect Subgroup 1	Keratoconus-Suspect Subgroup 2
KMP normal	14.28	72.34	12.50	16.66
KMP suspect	53.57	27.65	43.75	66.66
KMP KC	32.14	0.00	43.75	16.66

KC = keratoconus; KMP = keratoconus match probability

Table 3. Receiver operating characteristic data for corneal parameters.

Parameter	Keratoconus-Suspect Group				Keratoconus-Suspect Subgroup 1				Keratoconus-Suspect Subgroup 2			
	AUC (%)	Sensitivity (%)	Specificity (%)	Cutoff Point	AUC (%)	Sensitivity (%)	Specificity (%)	Cutoff Point	AUC (%)	Sensitivity (%)	Specificity (%)	Cutoff Point
ARTavg	95.1	91.3	88.1	<512	96.7	92.7	89.8	<504	94	90.2	87.7	<515
TCT	94.9	88.6	85.9	<522	90	99.9	76.6	<522	78.1	99.2	65.3	<562
KMI	94.0	85.7	87.5	<0.721	96.9	90.0	91.1	<0.562	91.8	87.5	79.55	<0.709
TCT:CCT	93.5	90.8	95.1	<0.9943	84.3	86.4	78.2	<0.992	79.9	78.4	64.2	<0.993
CRF	93.1	89	93.2	<8.9	94.5	92.73	84.5	<8.9	84.6	80	78.7	<8.8
PEL	92.3	84.1	89.8	>6	94.1	88.9	90.1	>8	90.8	79.3	87.6	>6
CH	90.4	88.5	88	<9.8	92.6	92.3	89.1	<9.3	82.7	85.3	85.1	<9.3
CCT	90.4	81.8	87.1	<529	90.1	99.8	78.7	<519	73.2	99.8	64.2	<565
PPIavg	85.3	81.1	78.2	>0.9	86.8	82.2	80.6	>0.9	82.8	79.4	74.2	>0.9
CV3	84.3	90.8	62.4	<3.9	85.8	91.2	64.1	<3.7	78.1	85.1	51.3	<4.1
CV5	81.4	59.8	90.1	<10.5	82.1	60.4	92.3	<9.8	77.2	56.4	88.5	<10.6

ARTavg = TCT/PPIavg; AUC = area under the receiver operating curve; CCT = central corneal thickness; CH = corneal hysteresis; CRF = corneal resistance factor; CV3 = corneal volume at 3.0 mm; CV5 = corneal volume at 5.0 mm; KMI = keratoconus match index; PEL = posterior elevation; PPIavg = average pachymetric progression index; TCT = thinnest corneal thickness; TCT:CCT = TCT:CCT ratio

explore the diagnostic capacity of the aforementioned parameters in the detection of keratoconus and keratoconus suspect, alone or in combination with anterior segment topographic and tomographic parameters.¹⁶⁻²⁰ However, despite recent progress in the detection of keratoconus suspect, universally accepted diagnostic criteria have yet to be developed.¹²

The updated software of the Ocular Response Analyzer (software 3.x) introduced 2 new

keratoconus-specific indices. These parameters, KMI and KMP, are the mathematical representations of waveform shape characteristics of the analyzer. According to the user's manual, each measurement signal

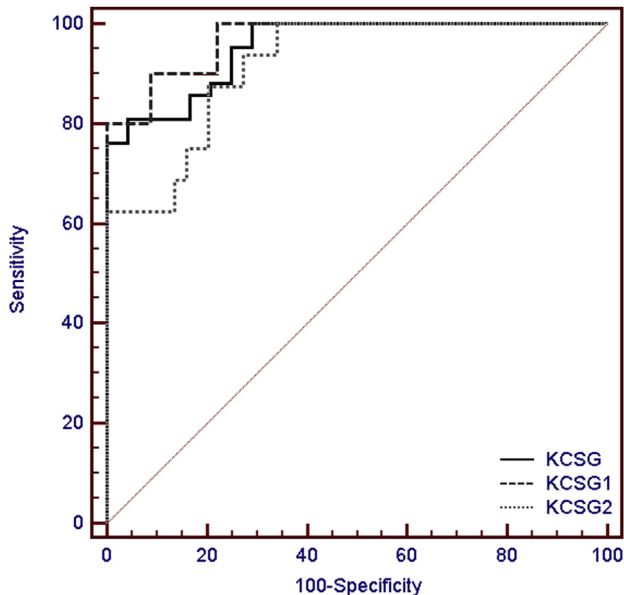


Figure 1. Receiver operating characteristic analysis of the KMI in keratoconus-suspect eyes (KCSG = keratoconus-suspect group; KCSG1 = keratoconus-suspect subgroup 1; KCSG2 = keratoconus-suspect subgroup 2).

Table 4. Spearman analysis between KMI and biomechanical and topographic data.

Parameter	r Value	P Value
K1 anterior (D)	0.13	.50
K2 anterior (D)	0.14	.47
Kmean anterior (D)	0.13	.48
K1 posterior (D)	-0.17	.37
K2 posterior (D)	-0.16	.39
Kmean posterior (D)	-0.18	.35
CCT	0.26	.17
TCT	0.30	.11
ISV	-0.007	.96
IVA	-0.06	.76
KI	-0.11	.55
CKI	-0.07	.70
IHA	-0.02	.91
IHD	-0.20	.29
Rmin	-0.12	.53
CH (mm Hg)	0.27	.15
CRF (mm Hg)	0.41	.03*

CCT = central corneal thickness; CH = corneal hysteresis; CKI = central keratoconus index; CRF = corneal resistance factor; IHA = index of height asymmetry; IHD = index of height decentration; ISV = index of surface variance; IVA = index of vertical asymmetry; K1 = keratometry in flat meridian; K2 = keratometry in steep meridian; KI = keratoconus index; Kmean = mean keratometry value; Rmin = smallest radius; TCT = thinnest corneal thickness

*Significant correlation

generates 37 waveform parameters scores. Because certain eye pathologies are supposed to share common waveform patterns, theoretically they could be classified according to their biomechanical properties.

The KMI index is derived from 7 waveform scores, representing the similarity of the waveform of the examined eye against the average waveform scores of keratoconus eyes in the machine's database. Apart from unpublished reports that suggest that normal KMI values are approximately 1 and keratoconus KMI values approximately 0, only 1 study of this new parameter was found in the international literature.²¹ That study's data indicated a mean KMI value of 0.98 in nonectatic (control) corneas and of 0.20 in keratoconic corneas, which is close to values in the unpublished reports. Moreover, the KMI had a high diagnostic capacity (overall predictive accuracy 97.7%) in keratoconic eyes, as indicated by the ROC analysis.²¹

In this study, we attempted to determine the KMI's diagnostic capacity in keratoconus-suspect eyes, which are known to present greater diagnostic challenges than keratoconic eyes, especially in refractive surgery settings. Our results suggest that the KMI differed significantly between control eyes and keratoconus-suspect eyes, while ROC curve analysis of the KMI indicated an overall predictive accuracy of 94%. The optimum cutoff point was estimated at 0.721, which means that corneas with KMI values below this point most likely represent cases of ectasia. The KMI results from keratoconus-suspect patients are consistent with our published results from keratoconus patients.²¹ The optimum KMI cutoff point of 0.721 is between 0.94, which represent nonectatic (control) corneas, and 0.46, which represents keratoconus stage 1 corneas according to the Amsler-Krumeich criteria.²¹ The clinical explanation of our results is that any KMI value below 0.721 is likely to represent subclinical keratoconus. Within the keratoconus disease continuum, as the KMI progresses to 0.46, the more likely it is for keratoconus to develop. Moreover, because keratoconus is associated with progressive corneal thinning, corneas with subclinical keratoconus and relatively low TCT measurements present KMI values closer to 0.46.

Regarding the potential association of the KMI with the pool of biomechanical and topographic parameters that we measured in our study, only the CRF had a significant correlation. Possibly, the CRF more efficiently reflects early biomechanical alterations of ectatic corneas; therefore, it is more strongly associated with the KMI. Regarding the impact of corneal thickness on the KMI, the mean values were not statistically significantly lower for thinner corneas (keratoconus-suspect subgroup 1) than for thicker corneas (keratoconus-suspect subgroup 2) (0.33 ± 0.51 versus 0.51

± 0.24) ($P = .059$, Mann-Whitney U test). Possibly, this difference would be statistically significant in a larger sample of patients.

On the other hand, the KMP index represents the probability that a cornea is normal, suspect, or ectatic. In addition, it differentiates ectatic corneas into mild, moderate, and severe cases. In our study, the KMP index returned no false-positive results in the control group; however, it classified 27.65% as suspect while 32.14% of keratoconus-suspect eyes were characterized as definite keratoconus. Regarding the high percentage of KMP suspect eyes in the normal group, one could speculate that Ocular Response Analyzer's software detected cases of subclinical keratoconus that could not be diagnosed by consecutive topographies and the calculation of the KISA% index that were performed in our normal group.

Nevertheless, we believe that the high percentage of suspect eyes in the normal population probably reflects an insufficiency of the index that limits its clinical value in differentiating keratoconus-suspect corneas from normal corneas. On the other hand, the relatively high percentage of KMP-derived normal eyes in our keratoconus-suspect group indicates the necessity of a prospective study that will determine whether keratoconus-suspect eyes will develop keratoconus (ie, KMP returns false negative results) or not develop it (KMP returns true negative results).

In conclusion, to our knowledge, this is the first study to evaluate the diagnostic potential of the new keratoconus-related Ocular Response Analyzer indices in keratoconus suspects. We found that the KMI had significant differentiating capacity, while the KMP did not fit very well with our study groups. Further studies with larger cohorts are necessary to confirm our results and further explore the diagnostic potential of these new parameters.

WHAT WAS KNOWN

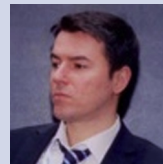
- The early detection of keratoconus suspects remains challenging.
- The diagnostic and differentiating capacity of 2 new keratoconus-related diagnostic indices (KMI and KMP) in keratoconus-suspect eyes is yet to be explored.

WHAT THIS PAPER ADDS

- The KMI seemed to effectively discriminate between keratoconus-suspect eyes and normal eyes.
- The KMP index had limited diagnostic value because it poorly differentiated between keratoconus-suspect corneas and normal corneas.

REFERENCES

1. Kennedy RH, Bourne WM, Dyer JA. A 48-year clinical and epidemiologic study of keratoconus. *Am J Ophthalmol* 1986; 101:267–273
2. Rabinowitz YS. Keratoconus. *Surv Ophthalmol* 1987; 42:297–319. Available at: <http://www.keratoconus.com/resources/Major+Review-Keratoconus.pdf>. Accessed October 12, 2013
3. Wilson SE, Klyce SD. Screening for corneal topographic abnormalities before refractive surgery. *Ophthalmology* 1994; 101:145–152
4. Nesburn AB, Bahri S, Salz J, Rabinowitz YS, Maguen E, Hofbauer J, Berlin M, Macy JI. Keratoconus detected by video-keratography in candidates for photorefractive keratectomy. *J Refract Surg* 1995; 11:194–201
5. Zadnik K, Barr JT, Edrington TB, Everett DF, Jameson M, McMahon TT, Shin JA, Sterling JL, Wagner H, Gordon MO; and the Collaborative Longitudinal Evaluation of Keratoconus (CLEK) Study Group. Baseline findings in the Collaborative Longitudinal Evaluation of Keratoconus (CLEK) Study. *Invest Ophthalmol Vis Sci* 1998; 39:2537–2546. Available at: <http://www.iovs.org/content/39/13/2537.full.pdf>. Accessed October 12, 2013
6. Ambrósio R Jr, Klyce SD, Wilson SE. Corneal topographic and pachymetric screening of keratorefractive patients. *J Refract Surg* 2003; 19:24–29
7. Holland DR, Maeda N, Hannush SB, Riveroll LH, Green MT, Klyce SD, Wilson SE. Unilateral keratoconus; incidence and quantitative topographic analysis. *Ophthalmology* 1997; 104:1409–1413
8. Saad A, Gatinel D. Topographic and tomographic properties of forme fruste keratoconus corneas. *Invest Ophthalmol Vis Sci* 2010; 51:5546–5555. Available at: <http://www.iovs.org/content/51/11/5546.full.pdf>. Accessed October 11, 2013
9. Bühren J, Kook D, Yoon G, Kohnen T. Detection of subclinical keratoconus by using corneal anterior and posterior surface aberrations and thickness spatial profiles. *Invest Ophthalmol Vis Sci* 2010; 51:3424–3432. Available at: <http://www.iovs.org/content/51/7/3424.full.pdf>. Accessed October 11, 2013
10. Bühren J, Kühne C, Kohnen T. Defining subclinical keratoconus using corneal first-surface higher-order aberrations. *Am J Ophthalmol* 2007; 143:381–389
11. de Sanctis U, Loiacono C, Richiardi L, Turco D, Mutani B, Grignolo FM. Sensitivity and specificity of posterior corneal elevation measured by Pentacam in discriminating keratoconus/subclinical keratoconus. *Ophthalmology* 2008; 115:1534–1539
12. Schlegel Z, Hoang-Xuan T, Gatinel D. Comparison of and correlation between anterior and posterior corneal elevation maps in normal eyes and keratoconus-suspect eyes. *J Cataract Refract Surg* 2008; 34:789–795
13. Ortiz D, Piñero D, Shabayek MH, Arnalich-Montiel F, Alió J. Corneal biomechanical properties in normal, post-laser in situ keratomileusis, and keratoconic eyes. *J Cataract Refract Surg* 2007; 33:1371–1375
14. Edmund C. Corneal elasticity and ocular rigidity in normal and keratoconic eyes. *Acta Ophthalmol Copenh* 1988; 66:134–140
15. Luce DA. Determining in vivo biomechanical properties of the cornea with an ocular response analyzer. *J Cataract Refract Surg* 2005; 31:156–162
16. Schweitzer C, Roberts CJ, Mahmoud AM, Colin J, Maurice-Tison S, Keratret J. Screening of forme fruste keratoconus with the Ocular Response Analyzer. *Invest Ophthalmol Vis Sci* 2010; 51:2403–2410. Available at: <http://www.iovs.org/content/51/5/2403.full.pdf>. Accessed October 11, 2013
17. Shah S, Laiquzzaman M, Bhojwani R, Mantry S, Cunliffe I. Assessment of the biomechanical properties of the cornea with the Ocular Response Analyzer in normal and keratoconic eyes. *Invest Ophthalmol Vis Sci* 2007; 48:3026–3031. Available at: <http://www.iovs.org/cgi/reprint/48/7/3026>. Accessed October 11, 2013
18. Kozobolis V, Sideroudi H, Giarmoukakis A, Gkika M, Labiris G. Corneal biomechanical properties and anterior segment parameters in forme fruste keratoconus. *Eur J Ophthalmol* 2012; 22:920–930
19. Saad A, Lteif Y, Azan E, Gatinel D. Biomechanical properties of keratoconus suspect eyes. *Invest Ophthalmol Vis Sci* 2010; 51:2912–2916. Available at: <http://www.iovs.org/content/51/6/2912.full.pdf>. Accessed October 11, 2013
20. Luz A, Fontes B, Ramos IC, Lopes B, Correia F, Schor P, Ambrósio R Jr. Evaluation of ocular biomechanical indices to distinguish normal from keratoconus eyes. *Int J Kerat Ect Cor Dis* 2012; 1:145–150. Available at: http://www.jaypeejournal.com/eJournals/ShowText.aspx?ID=4127&Type=FREE&TYP=TOP&IN=_eJournals/images/JPLGO.gif&IID=323&isPDF=YES. Accessed October 11, 2013
21. Labiris G, Gatziofufas Z, Sideroudi H, Giarmoukakis A, Kozobolis V, Seitz B. Biomechanical diagnosis of keratoconus: evaluation of the keratoconus match index and the keratoconus match probability. *Acta Ophthalmol Acta Ophthalmol* 2013; 91:e258–e262
22. Piñero DP, Alió JL, Alesón A, Escaf Vergara M, Miranda M. Corneal volume, pachymetry, and correlation of anterior and posterior corneal shape in subclinical and different stages of clinical keratoconus. *J Cataract Refract Surg* 2010; 36:814–825
23. Kovács I, Miháltz K, Németh J, Nagy ZZ. Anterior chamber characteristics of keratoconus assessed by rotating Scheimpflug imaging. *J Cataract Refract Surg* 2010; 36:1101–1106
24. Rabinowitz YS, Rasheed K. KISA% index: a quantitative video-keratography algorithm embodying minimal topographic criteria for diagnosing keratoconus. *J Cataract Refract Surg* 1999; 25:1327–1335; errata, 2000; 26:480



First author:

Georgios Labiris, MD, PhD

*Ophthalmology Department,
University Hospital of Alexandroupolis,
Alexandroupolis, Greece*